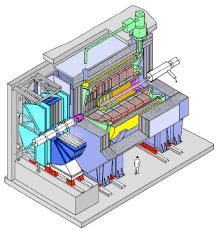

Physics Results from the H1 Experiment at HERA

Inclusive Measurements

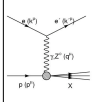

Deep inelastic scattering (DIS) at HERA proceeds via virtual boson exchange in Neutral Current, NC (left) and Charged Current, CC (right) interactions. Previous H1 measurements of the production cross sections of these processes have extracted the various proton structure functions and shown the respective cross sections to be of the same order at the electroweak unification scale.

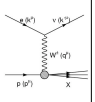

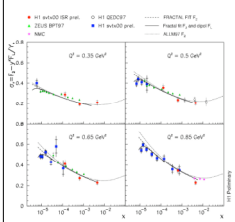

The inclusive DIS cross section is measured by H1 at low four momentum transfer Q^2 and relatively large Bjorken x using events with initial state photon radiation from the incoming electron. A compilation of low Q^2 measurements of the reduced cross section is shown on the left. Exploiting the new polarised lepton beam at HERA II, the dependence of the total e^-p and e^+p CC cross section on beam polarisation is shown as measured by H1 on the right, compared to the H1 PDF 2000 fit.

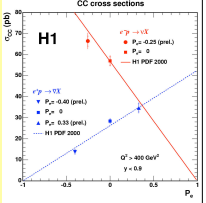

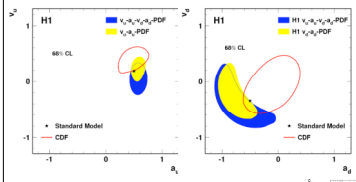

At high Q^2 the NC interactions receive contributions from gamma-Z^0 interference and Z^0 exchange. The high Q^2 e^+p H1 data are used to extract the axial and vector weak couplings of up and down quarks to the Z^0 boson. The results at 68% C.L. of PDF fits to the data are presented for the u quark (far left) and d quark (left), and compared to results recently obtained by the CDF experiment.

New H1 measurements of the inclusive charm and beauty cross sections at HERA are performed by exploiting the displacement of tracks from the primary vertex using precise spatial information from the H1 vertex detector. The measured charm and beauty structure functions $F_2^{c\bar{c}}$ and $F_2^{b\bar{b}}$ are shown left and far left respectively, in bins of Q^2 ranging from 3.5 GeV^2 to 650 GeV^2 and are compared to QCD predictions. Also shown for charm are the H1 and ZEUS measurements from D* meson analyses.

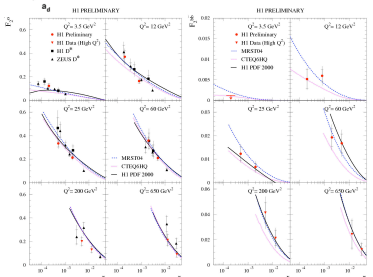

Rare Processes and Searches

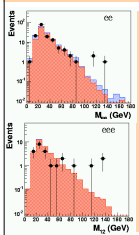

Multi electron production at HERA is studied using 163 pb^{-1} of H1 data. The distributions on the left show the reconstructed di-electron and tri-electron masses compared to the SM prediction; 3 "ee" and 3 "eee" events are observed compared to SM predictions of 0.44 ± 0.1 and 0.31 ± 0.08 respectively. The plot on the right shows the hadronic transverse momentum (P_T^X) distribution of events containing an isolated electron or muon and large missing transverse momentum, studied at H1 using 211 pb^{-1} of HERA data. At $P_T^X > 25$ GeV, 17 events are observed compared to a SM expectation of 6.4 ± 1.1.

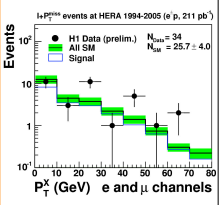

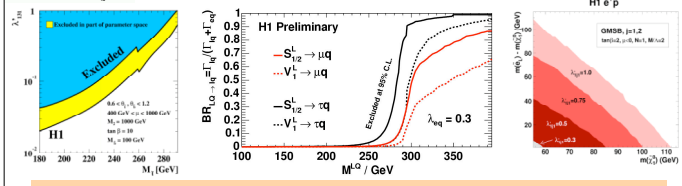

In a search for bosonic stop production no evidence is found, and stop masses up to 175 GeV for an em coupling strength are excluded, as shown in the above left plot. A search for lepton flavour violating processes mediated by leptoquarks finds no significant deviation from the Standard Model. The centre plot above shows mass limits on scalar and vector leptoquarks at 95% C.L. The above right plot shows excluded neutralino masses in a search for light gravitinos for various coupling strengths. This analysis presents the first HERA limits on R-parity violating SUSY independent of the squark sector.

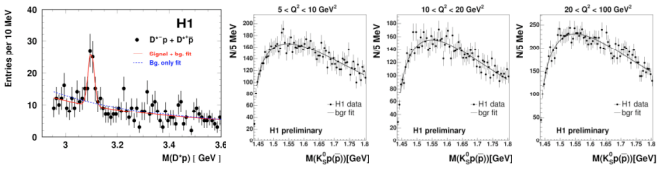

A narrow resonance in D^*p and $D^{*+}\bar{p}$ invariant mass combinations is observed by H1 in elastic e^+p collisions at HERA. The resonance has a mass of 3099 ± 3 (stat.) ± 5 (syst.) MeV, as shown in the above left figure, and is interpreted as an anti-charmed baryon with a minimal constituent quark composition $uudd\bar{c}$, together with the charge conjugate. A search for the strange pentaquark decaying to K_s^0p is performed at H1, where no significant signal is observed. The analysis mass spectra are displayed above in three bins of Q^2, together with a background function fit to the data.

Hadronic Final States

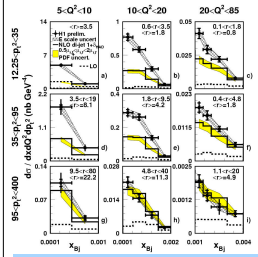

New parton dynamics, characterized by an initial state cascade which is non-ordered in parton virtuality, are expected to become important in the kinematic region of small Bjorken x in ep scattering at HERA. HI studies events with a forward jet, a region which typically lies away from the photon end of the evolution ladder. The figure on the left displays the hadron level triple differential cross section as a function of x in bins of Q^2 and $p_{T,jet}^2$. The data are compared to the prediction of NLO calculations, where the coloured band illustrates the scale uncertainty in the calculations; the band following the data points indicates the energy scale uncertainty.

Deep inelastic e^+p scattering data taken with the H1 detector at HERA are used to investigate jet production over a range of four momentum transfers $150 < Q^2 < 15000$ GeV^2 and transverse jet energies $5 < E_T < 50$ GeV. The ratio of the tri-jet to the di-jet cross section is used to extract the value and evolution of the strong coupling constant as a function of Q^2, as shown on the right. The value of the strong coupling constant determined from the study is 0.1175 ± 0.0017 (stat.) ± 0.0050 (syst.) +0.0054 -0.0068 (theory), which compares well with the world average.

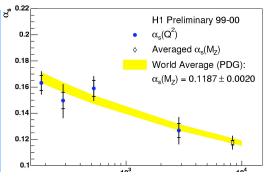

The cross sections for photoproduction events that contain a D* and a jet are measured by H1 to investigate the charm production mechanism. The figure on the right shows the cross section in bins of the phi separation of the D* and jet compared to NLO calculations with and without hadronisation corrections.

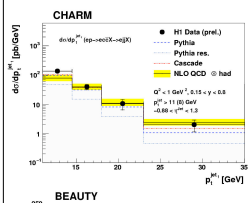

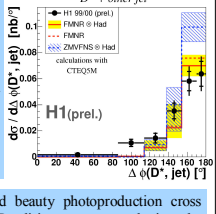

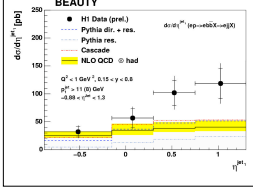

A measurement of the charm and beauty photoproduction cross section is performed using high P_T di-jet events, employing the lifetime signature of c and b flavoured hadrons to determine the fraction of events containing charm or beauty. The upper left plot shows the differential charm cross section as a function of transverse momentum of the leading jet, which extends to higher P_T than previous D* analyses. The lower left plot shows the differential beauty cross section as a function of pseudo rapidity of the leading jet, where an excess of data over the NLO QCD prediction is observed in the forward direction.

Diffraction

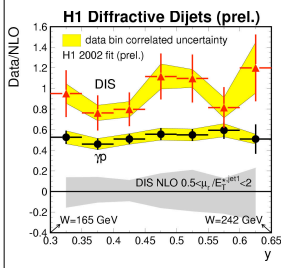

H1 performs measurements of differential dijet cross sections in low-|t| diffractive photoproduction ($Q^2 < 0.01$ GeV^2) and deep inelastic scattering ($Q^2 > 4$ GeV^2). The measurements of dijet rates in photoproduction and DIS are compared with NLO QCD predictions based on diffractive parton distributions previously obtained from a NLO QCD analysis of inclusive diffractive DIS. Whereas the diffractive dijet rate in DIS is in good agreement with QCD factorisation, the dijet rate in photoproduction is suppressed by about a factor 0.5 compared to the NLO QCD prediction, as can be seen in the figure on the left. The preliminary results are suggestive of a breakdown of factorisation in photoproduction for both direct and resolved photon interactions.

Total and differential charged current cross sections in Q^2 (shown on the right), x_{pom} and beta are measured by H1 in the kinematic range $Q^2 > 200$ GeV^2, $y < 0.9$ and $x_{pom} < 0.05$ and compared to a model where diffractive parton densities are extracted from fits to neutral current data at lower Q^2. The ratio of the diffractive charged current cross-section to the inclusive charged current cross-section is measured to be 2.5 ± 0.8 (stat.) ± 0.6 (syst.) %.

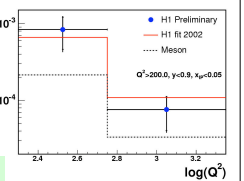

The diffractive photoproduction of rho mesons with large momentum transfer, is measured at H1. The measured t dependence of the cross section is shown on the left compared to a BFKL model. The diffractive photoproduction of high P_T photons is also measured at H1. The differential cross section as a function of -t is shown on the right and compared to a leading log BFKL model with different values of the strong coupling constant.

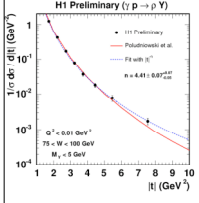

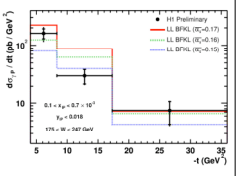

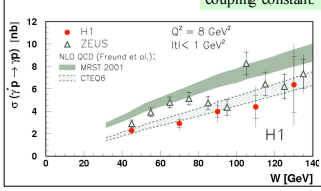

The elastic deeply virtual Compton scattering process is measured by H1 in the kinematic range $2 < Q^2 < 80$ GeV^2, $30 < W < 140$ GeV and $|t| < 1$ GeV^2. The measured cross section is shown as a function of W on the left, where the data are compared the ZEUS measurement and to NLO QCD predictions.